Statistical Damage Localization with Stochastic Load Vectors Using Multiple Mode Sets

Md Delwar Hossain Bhuyan, Michael Döhler, Laurent Mevel

Statistical Damage Localization with Stochastic Load Vectors Using Multiple Mode Sets

Md Delwar Hossain Bhuyan[1], Michael Döhler[1], Laurent Mevel[1]

[1] Inria/IFSTTAR, I4S team, Campus de Beaulieu, 35042 Rennes
md-delwar-hossain.bhuyan@inria.fr, michael.doehler@inria.fr, laurent.mevel@inria.fr

Keywords: Damage localization, Load vectors, Covariance analysis, Statistical analysis, Subspace method.

Abstract
The Stochastic Dynamic Damage Locating Vector (SDDLV) method is an output-only damage localization method based on both a Finite Element (FE) model of the structure and modal parameters estimated from output-only measurements in the damage and reference states of the system. A vector is obtained in the null space of the changes in the transfer matrix computed in both states and then applied as a load vector to the model. The damage localization is related to this stress where it is close to zero. In previous works an important theoretical limitation was that the number of modes used in the computation of the transfer function could not be higher than the number of sensors located on the structure. It would be nonetheless desirable not to discard information from the identification procedure. In this paper, the SDDLV method has been extended with a joint statistical approach for multiple mode sets, overcoming this restriction on the number of modes. The new approach is validated in a numerical application, where the outcomes for multiple mode sets are compared with a single mode set. From these results, it can be seen that the success rate of finding the correct damage localization is increased when using multiple mode sets instead of a single mode set.

1. INTRODUCTION

Vibration based damage localization has become an important issue for Structural Health Monitoring (SHM) such as bridges, buildings and offshore structures. Sensors installed on the structure collect data and then the modal parameters (damping ratios, natural frequencies and mode shapes) can be estimated. Those parameters are meaningful for the monitoring of the structure and damage localization is possible when updating these changes in a Finite Element (FE) model of the structure.

The SDDLV approach [1] is a vibration based damage localization technique using both finite element information and modal parameters estimated from output data. The estimates of the modal parameters are subject to variance errors [2–4]. Based on that uncertainty information, a statistical extension of the SDDLV method was developed in [5, 6] for deciding if an element is damaged.

In [5, 6], the number of modes used in the computation could not be bigger than the number of sensors located on the structure. This is a restriction when there are more modes describing the structure than the available sensors. Here, the SDDLV method is developed with a joint statistical evaluation using multiple mode sets. It overcomes this limitation. It is demonstrated that the computation of stress for multiple mode sets increases the information content about the damaged or non-damaged elements of the structure. Finally, all stress values corresponding to each element are being tested for damage in an hypothesis test where the computed stresses are evaluated with their joint covariance. To derive such a test, the computation of the covariance of the resulting stress is necessary. Following [7], the necessary covariance scheme is developed and extended for a joint statistical evaluation using multiple mode sets for the same or different Laplace variables.

Assessing the performance of the method is a requirement for showing the benefits of this approach. A proper criterion for the evaluation of the success rate is proposed based on Monte Carlo simulations.

The SDDLV approach is strongly dependent on the choice of the Laplace variable s where the transfer function is evaluated. Performance can be highly different in the classical SDDLV approach depending on the choice of the Laplace variable. Accommodating multiple s variables has been treated in [6]. Still, the choice of the Laplace variable is a complicated part of the procedure, even if past guidelines push for choosing this variable around the identified modes in the complex plane. That is why, in this paper, Monte Carlo simulations have been done for many s variables in the complex plane and results are evaluated on 2D grids. Performance of the proposed approach is tested against the requirement that such choice should not be critical.

This paper is formulated as follows. In Section 2, the SDDLV method is presented as a vibration-based damage localization approach. In Section 3, the effect of removing the limiting restriction on the number of modes will be discussed. In Section 4, the statistical damage localization approach is derived using multiple mode sets. In Section 5, the new approach is applied on a numerical application to evaluate the success rate of the localization, and conclusion of the work is presented in Section 6.

2. DAMAGE LOCALIZATION APPROACH (SDDLV)

The Stochastic Dynamic Damage Locating Vector (SDDLV) approach is an output-only damage localization method based on interrogating changes $\delta G(s)$ in the transfer matrix $G(s)$ of a system in both reference and damaged states [1]. A vector is obtained in the null space of $\delta G(s)$ from system identification results using output-only measurements corresponding to both states. Then this load vector is applied to the Finite Element (FE) model of the structure for the computation of a stress field over the structure. Damage localization is related to this stress field where the computed stress is zero or close to zero in practice [1, 8–10].

In this section, the deterministic computation of the stress field and the aggregation results is summarized, before deriving its statistical evaluation in Section 4.

2.1 Modeling of a mechanical structure

The behavior of a mechanical structure can be described by a linear time-invariant (LTI) dynamic system

$$M\ddot{\mathscr{X}}(t)+C_d\dot{\mathscr{X}}(t)+K\mathscr{X}(t)=f(t) \tag{1}$$

with M, C_d, $K \in \mathbb{R}^{d\times d}$ are the mass, damping and stiffness matrices respectively, where t indicates continuous time and $\mathscr{X} \in \mathbb{R}^d$ defines displacements of the d Degrees Of Freedom (DOF) of the structure. The external force $f(t)$ is not measurable and modeled as white noise. Let the dynamic system (1) be observed at r coordinates. Since $f(t)$ is unmeasured, it can be substituted with a fictive force $e(t) \in \mathbb{R}^r$ which is acting only in the measured coordinates and that regenerates the measured output. After replacing $x = [\mathscr{X} \quad \dot{\mathscr{X}}]^T$ with (1) leads to the corresponding continuous-time state-space model

$$\begin{cases} \dot{x} = A_c x + B_c e \\ y = C_c x + D_c e \end{cases} \tag{2}$$

with state vector $x \in \mathbb{R}^n$, output vector $y \in \mathbb{R}^r$, the state transition matrix $A_c \in \mathbb{R}^{n\times n}$ and output matrix $C_c \in \mathbb{R}^{r\times n}$, where $n = 2d$ is the system order and r is the number of outputs. Since input of the system is replaced by the fictive force $e \in \mathbb{R}^r$, the input influence matrix and direct transmission matrix are $B_c \in \mathbb{R}^{n\times r}$ and $D_c \in \mathbb{R}^{r\times r}$ respectively. However, only the system matrices A_c and C_c are relevant from output-only system identification and the non-identified matrices B_c and D_c will only be needed to obtain estimates of the transfer matrix. From Stochastic Subspace Identification (SSI) [11], estimates $\widehat{A}_c$ and $\widehat{C}_c$ can be obtained from output only measurements, details are given in [6].

2.2 Computation of damage indicator

The transfer matrix $G(s) \in \mathbb{C}^{r\times r}$ of system (2) can be derived as

$$G(s) = R(s)D_c, \quad \text{where} \quad R(s) = C_c(sI - A_c)^{-1} \begin{bmatrix} C_cA_c \\ C_c \end{bmatrix}^{\dagger} \begin{bmatrix} I \\ 0 \end{bmatrix} \tag{3}$$

for the restriction of the system order to $n \leq 2r$ which is described in details in [1,8]. s is a Laplace variable in the complex plane, I is the identity matrix of size r, 0 is zero matrix, and † denotes the Moore-Penrose pseudoinverse. The difference of the transfer matrices in both damaged (variables with tilde) and healthy states is $\delta G(s) = \tilde{G}(s) - G(s)$. The matrices $\delta G(s)$ and $\delta R^T(s) = \tilde{R}^T(s) - R^T(s)$ have the same null space [1]. The desired load vector $v(s)$ is obtained from the null space of the $\delta R^T(s)$ from Singular Value Decomposition (SVD)

$$\delta R^T(s) = U\Sigma V^H = \begin{bmatrix} U_1 & U_2 \end{bmatrix} \begin{bmatrix} \Sigma_1 & 0 \\ 0 & \Sigma_2 \end{bmatrix} \begin{bmatrix} V_1 & V_2 \end{bmatrix}^H, \tag{4}$$

where $U, \Sigma, V \in \mathbb{C}^{r\times r}$, $\Sigma_2 \approx 0$ and ^{H} indicates conjugate transpose. Let n_u be the dimension of image U_1 and $(r - n_u)$ be the dimension of the null space V_2, where n_u depends on kind and number of damaged elements [9]. Note that only output data is necessary for the computation of an estimate of $v(s)$. To compute the stress field, load vector $v(s)$ is applied to the FE model of the structure. This stress is obtained through a linear relation to $v(s)$ by the matrix $L_{model}(s) \in \mathbb{C}^{l\times r}$ from FE model of the structure [1,5] and satisfies

$$S(s) = L_{model}(s)v(s). \tag{5}$$

Theoretically, the stress vectors $S(s)$ indicate damage [1,9] where entries in $S(s)$ close to zero indicate potentially damaged elements. However, these stresses are not exactly zero but small in practice because of modal truncation, model errors and uncertainties from measurements.

2.3 Stress aggregation for robustness

Let the s-values s_x, $x = 1, \ldots, w$ be given. To minimize error, they should be chosen in the area of the identified poles of the system but not too close to them [1,6]. After identification of the system matrices in both states, the computations of (4)-(5) are repeated for each s_x to get the respective stress vectors $S(s_x)$. For multiple s-values, the stress aggregation is obtained for each entry j as follows [6]

$$\bar{S}_j = \sum_{x=1}^{w} |S_j(s_x)| \tag{6}$$

In Section 3, the theoretical limitation on number of modes is discussed and then in Section 4, a new statistical scheme is proposed using multiple mode sets while considering uncertainties of the results at the same time.

3. REMOVING THE RESTRICTION ON NUMBER OF MODES

In practice, there may be more modes available from identification than number of sensors on the structure. It will be meaningful to be able to utilize this information completely from the identification procedure. In [1], it was not possible to use all modes in that context due to theoretical restrictions, $n \leq 2r$ where $n = 2m$ is the system order and r is the number of sensors. Note that m is the number of conjugated complex mode pairs identified from datasets where m has to satisfy the constraint $m \leq r$.

In order to remove the restriction on the number of modes, the computation of stress from different mode sets is investigated. Note that for each mode set the current restriction needs to be satisfied. Now the computation of stress is developed at multiple mode sets by joint statistical approach which should increase the information content about damage localization on the structure.

For simplicity of the notation, consider only 2 sets of modes, while the following development can be easily generalized for arbitrary mode sets. Let $\mathscr{M} = (i, j)$ be two sets of modes of the system that contains m_i and m_j modes respectively with $n_i = 2m_i$ and $n_j = 2m_j$ being the respective model orders. In order to compute stress, the conditions $m_i \leq r$ and $m_j \leq r$ need to be satisfied. For each mode set, the system matrices are obtained using SSI performed on the same measurement in the healthy and damaged states [6]. The "transfer matrix" resultant $R(s)$ in (4) is computed from both states and the stress vector is obtained separately for the respective load vector. For each mode set i and j, the system matrices A_c^i, C_c^i and A_c^j, C_c^j are computed and subsequently "transfer matrix" results $R^i(s)$, $R^j(s)$ are also computed. Then different load vectors are obtained as $v^i(s)$ and $v^j(s)$ from the same measurement data for the respective mode sets i and j. They are respectively applied to model for stress computation and it yields $S^i(s) = L_{model}(s)v^i(s)$ and $S^j(s) = L_{model}(s)v^j(s)$. Then both stresses $S^i(s)$ and $S^j(s)$ are used for joint stress evaluation.

There is a possibility to use same or different s-values for each of the stress. For simplicity, one s-value s_i is used for mode set i and s_j for mode set j and then $S^i(s_i)$ and $S^j(s_j)$ are computed. However, it can also be easily generalized for several s-values. Now, several stress values are calculated because of multiple mode sets and hence, robustness of the damage localization can be obtained by aggregating the stress results.

4. UNCERTAINTIES PROPAGATION AND COVARIANCE COMPUTATION

For the damage localization algorithm, estimates of the system matrices A_c and C_c are obtained in the damaged and undamaged states from limited data lengths using SSI [6]. The identification of system matrices are subject to variance errors because of unknown excitation, measurement noise and limited data length. The uncertainties in the estimates are penalizing the quality and precision of the damage localization results. For making decisions about damaged elements of the structure, these uncertainties need to be used to decide whether stress of an element is significantly zero or not. In [5, 6], uncertainty quantification of the stress vector $S(s)$ in (5) was computed for a single mode set at one or several s-values. In this section, uncertainty computation of the stress vector $S^{\mathscr{M}}(s)$ is derived for two mode sets $\mathscr{M}$, though it can also be easily generalized to any number of mode sets.

All parameters derived in this method are estimated from measurement data through the computation of the H matrix, which is the Hankel matrix of the cov-SSI method. Details are given in [5, 7].

Let $\hat{\Sigma}_H$ be the covariance of $vec(H)$ and f be a function of H that is estimated from data. Its covariance can be approximated by

$$cov(f(H)) \approx \mathscr{J}_{f,H} \hat{\Sigma}_H \mathscr{J}_{f,H}^T. \tag{7}$$

Note that sensitivity $\mathscr{J}_{f,H} = \partial f(H) / \partial vec(H)$ in the above derivation. From perturbation theory, a first-order perturbation $\triangle f$ is defined by $\triangle$ operator of the function f, which gives

$$\triangle f = \mathscr{J}_{f,H} vec(\triangle H). \tag{8}$$

With this relationship, the desired sensitivity can be computed from (8) and then it can be used for covariance computation in (7). The $vec(.)$ defines the column stacking vectorization operator. Since the Hankel matrix is dependent on datasets, the estimated covariance $\hat{\Sigma}_H$ of the Hankel matrix H estimate can be propagated to any parameters, particularly to the modal parameters and stress estimate $\hat{S}(s)$.

Note that some of the matrices are complex-valued variable in Section 4.1. To deal with uncertainties of the complex-valued matrices, define an equivalent real-valued notation for any matrix Q as follows

$$\mathrm{Q}_{Re} \stackrel{\text{def}}{=} \begin{bmatrix} \mathrm{Real(Q)} & -\mathrm{Imag(Q)} \\ \mathrm{Imag(Q)} & \mathrm{Real(Q)} \end{bmatrix}, \mathrm{Q}_{re} \stackrel{\text{def}}{=} \begin{bmatrix} \mathrm{Real(Q)} \\ \mathrm{Imag(Q)} \end{bmatrix}$$

Now, for multiple mode sets i and j, the covariance of the system matrices can be derived as follows

$$\Sigma_{A_c^i,C_c^i} \stackrel{\text{def}}{=} \begin{bmatrix} \mathscr{J}_{A_c^i,H} \\ \mathscr{J}_{C_c^i,H} \end{bmatrix} \Sigma_H \begin{bmatrix} \mathscr{J}_{A_c^i,H} \\ \mathscr{J}_{C_c^i,H} \end{bmatrix}^T, \Sigma_{A_c^j,C_c^j} \stackrel{\text{def}}{=} \begin{bmatrix} \mathscr{J}_{A_c^j,H} \\ \mathscr{J}_{C_c^j,H} \end{bmatrix} \Sigma_H \begin{bmatrix} \mathscr{J}_{A_c^j,H} \\ \mathscr{J}_{C_c^j,H} \end{bmatrix}^T \tag{9}$$

where $\mathscr{J}_{A_c^i,H}$, $\mathscr{J}_{C_c^i,H}$ and $\mathscr{J}_{A_c^j,H}$, $\mathscr{J}_{C_c^j,H}$ are the sensitivity of the system matrices for mode sets i and j respectively and details are given in [3, 6, 7] for subspace identification.

4.1 Covariance computation of the stress vector $S(s)$

For stress variance computation, the sensitivity $\mathscr{J}_{R(s),(A_c,C_c)}$ of the matrix $R(s)$ in (3) with respect to the system matrices A_c and C_c was derived in [5, 6]. The covariance of the matrices $R(s)$ and $\tilde{R}(s)$ are computed in the damaged and healthy states of the structure for a chosen s-value. These covariances are propagated to the load vector $v(s)$ that belongs to the null space of $\delta R^T(s) = \tilde{R}^T(s) - R^T(s)$ and subsequently propagated to the stress vector $S(s)$.

For multiple mode sets $\mathscr{M} = (i, j)$, the sensitivity $\mathscr{J}^{\mathscr{M}}_{v(s),\delta R^T}$ of the load vector $v(s)$ with respect to δR^T is computed based on $\triangle v^{\mathscr{M}}(s)_{re} = \mathscr{J}^{\mathscr{M}}_{v(s),\delta R^T}(vec(\triangle \delta R(s)^T))^{\mathscr{M}}_{re}$ with [5, Proposition 4] and then it follows from (5)

$$\triangle S^{\mathscr{M}}(s)_{re} = \mathscr{J}^{\mathscr{M}}_{S(s),\delta R^T}(vec(\triangle \delta R^T(s)))^{\mathscr{M}}_{re},$$

where $\mathscr{J}^{\mathscr{M}}_{S(s),\delta R^T} \stackrel{\text{def}}{=} (L_{model(s)})_{Re}\mathscr{J}^{\mathscr{M}}_{v(s),\delta R^T}$. The above expression can be derived as in [5, Theorem 5]. For multiple mode sets $\mathscr{M}$, the above expression can be written for covariance computation of $S^{\mathscr{M}}(s)$ in the selection of different mode sets i and j respectively

$$\begin{aligned} \triangle S^{\mathscr{M}}(s)_{re} &= \mathscr{J}^{\mathscr{M}}_{S(s),\delta R^T}\mathscr{J}^{\mathscr{M}}_{\tilde{R}(s),(\tilde{A}_c,\tilde{C}_c)} \begin{bmatrix} vec(\triangle \tilde{A}_c^{\mathscr{M}}) \\ vec(\triangle \tilde{C}_c^{\mathscr{M}}) \end{bmatrix} - \mathscr{J}^{\mathscr{M}}_{S(s),\delta R^T}\mathscr{J}^{\mathscr{M}}_{R(s),(A_c,C_c)} \begin{bmatrix} vec(\triangle A_c^{\mathscr{M}}) \\ vec(\triangle C_c^{\mathscr{M}}) \end{bmatrix} \\ &= \tilde{\mathscr{J}}^{\mathscr{M}}_{S(s),(\tilde{A}_c,\tilde{C}_c)}\tilde{\mathscr{J}}^{\mathscr{M}}_{(\tilde{A}_c,\tilde{C}_c),\tilde{H}} vec(\triangle \tilde{H}) - \mathscr{J}^{\mathscr{M}}_{S(s),(A_c,C_c)}\mathscr{J}^{\mathscr{M}}_{(A_c,C_c),H} vec(\triangle H) \end{aligned} \tag{10}$$

with $\tilde{\mathscr{J}}^{\mathscr{M}}_{S(s),(\tilde{A}_c,\tilde{C}_c)} \stackrel{\text{def}}{=} \mathscr{J}^{\mathscr{M}}_{S(s),\delta R^T}\mathscr{J}^{\mathscr{M}}_{\tilde{R}(s),(\tilde{A}_c,\tilde{C}_c)}$, $\tilde{\mathscr{J}}^{\mathscr{M}}_{(\tilde{A}_c,\tilde{C}_c),\tilde{H}} \stackrel{\text{def}}{=} \begin{bmatrix} \mathscr{J}_{\tilde{A}_c^{\mathscr{M}},\tilde{H}} \\ \mathscr{J}_{\tilde{C}_c^{\mathscr{M}},\tilde{H}} \end{bmatrix}$, $\mathscr{J}^{\mathscr{M}}_{S(s),(A_c,C_c)} \stackrel{\text{def}}{=} \mathscr{J}^{\mathscr{M}}_{S(s),\delta R^T}\mathscr{J}^{\mathscr{M}}_{R(s),(A_c,C_c)}$

and $\mathscr{J}^{\mathscr{M}}_{(A_c,C_c),H} \stackrel{\text{def}}{=} \begin{bmatrix} \mathscr{J}_{A_c^{\mathscr{M}},H} \\ \mathscr{J}_{C_c^{\mathscr{M}},H} \end{bmatrix}$.

After stacking the real and imaginary parts of the stress vector $S^{\mathscr{M}}(s)$ for multiple mode sets $\mathscr{M} = (i, j)$, the total stress vector is derived as follows

$$S(s) \stackrel{\text{def}}{=} \begin{bmatrix} S^i(s)_{re} \\ S^j(s)_{re} \end{bmatrix}. \tag{11}$$

For multiple mode sets $\mathscr{M} = (i, j)$, $\triangle S^i(s)$ and $\triangle S^j(s)$ can be derived separately with (10). After stacking all mode sets accordingly, it follows

$$\triangle S(s) = \begin{bmatrix} \tilde{\mathscr{J}}^i_{S(s),(\tilde{A}_c,\tilde{C}_c)}\tilde{\mathscr{J}}^i_{(\tilde{A}_c,\tilde{C}_c),\tilde{H}} \\ \tilde{\mathscr{J}}^j_{S(s),(\tilde{A}_c,\tilde{C}_c)}\tilde{\mathscr{J}}^j_{(\tilde{A}_c,\tilde{C}_c),\tilde{H}} \end{bmatrix} vec(\triangle \tilde{H}) - \begin{bmatrix} \mathscr{J}^i_{S(s),(A_c,C_c)}\mathscr{J}^i_{(A_c,C_c),H} \\ \mathscr{J}^j_{S(s),(A_c,C_c)}\mathscr{J}^j_{(A_c,C_c),H} \end{bmatrix} vec(\triangle H)\ . \tag{12}$$

Then covariance of the stress can be defined as $cov(vec(S(s))) \stackrel{\text{def}}{=} \Sigma_{S(s)}$ and analytically, it yields

$$\begin{aligned} \Sigma_{S(s)} = &\begin{bmatrix} \tilde{\mathscr{J}}^i_{S(s),(\tilde{A}_c,\tilde{C}_c)}\tilde{\mathscr{J}}^i_{(\tilde{A}_c,\tilde{C}_c),\tilde{H}} \\ \tilde{\mathscr{J}}^j_{S(s),(\tilde{A}_c,\tilde{C}_c)}\tilde{\mathscr{J}}^j_{(\tilde{A}_c,\tilde{C}_c),\tilde{H}} \end{bmatrix} \Sigma_{\tilde{H}} \begin{bmatrix} \tilde{\mathscr{J}}^i_{S(s),(\tilde{A}_c,\tilde{C}_c)}\tilde{\mathscr{J}}^i_{(\tilde{A}_c,\tilde{C}_c),\tilde{H}} \\ \tilde{\mathscr{J}}^j_{S(s),(\tilde{A}_c,\tilde{C}_c)}\tilde{\mathscr{J}}^j_{(\tilde{A}_c,\tilde{C}_c),\tilde{H}} \end{bmatrix}^T + \\ &\begin{bmatrix} \mathscr{J}^i_{S(s),(A_c,C_c)}\mathscr{J}^i_{(A_c,C_c),H} \\ \mathscr{J}^j_{S(s),(A_c,C_c)}\mathscr{J}^j_{(A_c,C_c),H} \end{bmatrix} \Sigma_H \begin{bmatrix} \mathscr{J}^i_{S(s),(A_c,C_c)}\mathscr{J}^i_{(A_c,C_c),H} \\ \mathscr{J}^j_{S(s),(A_c,C_c)}\mathscr{J}^j_{(A_c,C_c),H} \end{bmatrix}^T. \end{aligned} \tag{13}$$

The covariance expression (13) yields a new statistical approach for damage localization using multiple mode sets based on a statistical test for each element t of the structure. In this approach, all stress components in S_t corresponding to an element t are being tested in a hypothesis test, where computed stress values are related to their joint covariance (13). Since an estimate of the stress vector S_t is asymptotically Gaussian distributed, a statistical evaluation is derived for each element t in a χ_t^2-test as

$$\chi_t^2 = S_t^T \Sigma_t^{-1} S_t. \tag{14}$$

5. APPLICATIONS

5.1 Test case

The damage localization method has been applied to a mass-spring chain system as shown in Figure 1. The total number of Degrees Of Freedom (DOF) of the structure is 6. The damaged element in the model is simulated by decreasing stiffness by 10 % of its original value. For damaged and undamaged states, the acceleration data length for each set is N = 50,000. Data were generated from collocated white noise excitation using three sensors at elements 2, 4 and 6 in Figure 1 with sampling frequency of 50 Hz, 2% damping ratio and 5% white noise were also added to the output data. In this example, 6 modes can be identified from model of the structure using SSI. A subset of 3 modes could be used in the previous works [6] as the number of modes could not be bigger than the number of output sensors. For the new method, the identified modes are splitted in two mode sets namely i and j of 3 modes each.

In the application, the outcome of the damage localization results using multiple mode sets are compared with using only a single mode set. Recall that stress values close to zero indicate potentially damaged elements. From SSI, all estimated modes were chosen using a stabilization diagram procedure [12]. Then, the system matrices in both reference and damaged states are computed [6] and for multiple mode sets, their variance is derived from the same dataset as described in Section 4.

Notice that there is always a possibility to use the same or different s-values for the computation of stress with the proposed method. Let the Laplace variable s_i and s_j be chosen within the range of the identified poles for mode sets i and j respectively. Then, real and imaginary parts of the stress vector and their joint covariance in (13) are computed for these Laplace variables s_i and s_j. Finally, 4 stress values are computed for each element t including real and imaginary parts of $S_t^i(s_i)$ and $S_t^j(s_j)$ for mode set i and j respectively. For each element t, these stress values are aggregated statistically in the χ_t^2-test.

5.2 Performance evaluation of damage localization

To analyse the performance of the proposed damage localization method using multiple mode sets, the results are compared with a single mode set experiment. 500 datasets are generated by Monte-Carlo simulations to evaluate the success rate of the damage localization. In order to indicate if an element is potentially damaged or not, the χ_t^2 value is computed for each element. Successful damage localization means that the lowest χ_t^2 value is at the damaged element. The success rate corresponds to the probability of detection or power of the test. Here, the success rate of the successful damage localization is defined as the number of occurrences of the smallest χ_t^2 values at damaged elements.

Figure 1: Mass-spring chain system (6 DOFs)

In order to see the influence of all s-values $s = (p, q) \in \mathbb{C}$, a grid map in the complex s-plane has been proposed. Let real and imaginary parts of the s-value be defined as p and q. Define $p = a : b : c$ while the discrete range [a, c] = [-3, 1] is chosen by using a step $b = 0.5$ and then $q = d : e : f$, when the discrete range [d, f]= [1, 130] is selected by step $e = 2$. The range of s-values has been chosen in the vicinity of the identified poles, $\lambda_c^i \in \mathbb{C}$ in Table 1. The χ_t^2-tests for all s-values are evaluated for each of the 500 datasets in order to evaluate the influence of different s-values. Then performance evaluation of the method is illustrated in a 3D-bar diagram where x-y axes indicate real-imaginary parts of s-value and z-axis corresponds to success rate of damage localization.

Table 1: Identified Poles

Mode i	1	2	3	4	5	6
$\lambda_c^i \in \mathbb{C}$	$(-0.25, 12.8)$	$(-0.74, 37.4)$	$(-1.16, 58.3)$	$(-1.56, 77.8)$	$(-1.96, 98.2)$	$(-2.13, 106.6)$

In Section 5.3, the damage localization results are demonstrated in all elements computed at one s-value for one data set. Then, success rate of the damage localization results has been computed using a single mode set in Monte-Carlo simulation for 500 data set in Section 5.4. Finally, the success rate of the damage localization results is illustrated with the new proposed method using multiple mode sets in Section 5.5.

5.3 Localization of results in all elements at one s-value

The localization tests at all elements are computed using one of the Monte-Carlo datasets only in both damaged and healthy states. Recall that the damage position is inferred by the stress value closest to zero. For a single mode set, the computation of all stresses is done at $s_1 = (-2, 51) \in \mathbb{C}$. In Figure 2(a), all stress values corresponding to healthy and damaged elements are presented, while the smallest stress value is correctly located in the damaged element at bar 4. In Figure 2(b), the estimated stress cannot correctly indicate the damage position, due to modal truncation and variance errors. Considering uncertainties, the damage position is correctly found at the smallest χ_t^2 values at element 4 in Figure 2(c). It can be seen that χ_t^2 in Figure 2(c) shows similar results as the theoretical result in Figure 2(a).

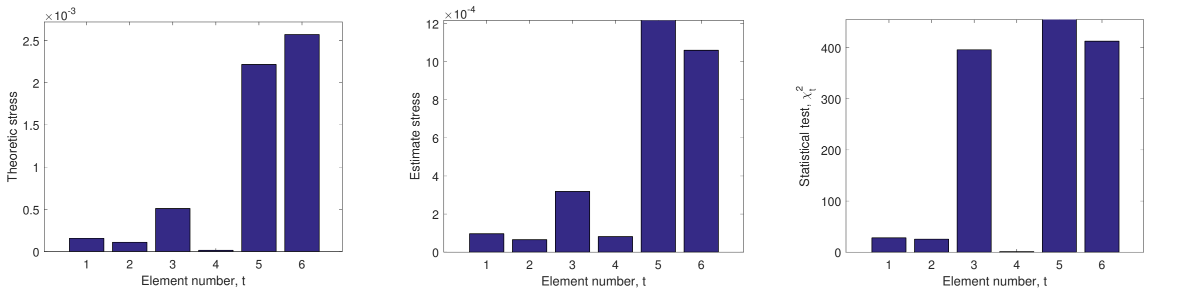

(a) Stress from exact modal parameters (b) Stress from estimates data sets (c) statistical evaluation of estimates data

Figure 2: Localization using a single mode set: stress computation and statistical evaluation at $s_1 = (-2, 51) \in \mathbb{C}$ -three sensors, 5% output noise, 10% stiffness reduction at bar 4.

5.4 Success rate of the damage localization using a single mode set

In this section, the damage localization results are illustrated in Figure 3 and Figure 4 for both single mode sets i and j comprising the first and last three modes respectively. All these computations are done at Laplace variables, $s = (p, q) \in \mathbb{C}$ (i.e. recall $p = 1 : 0.5 : -3$ and $q = 1 : 2 : 130$) which are located in the vicinity of the identified poles (see Table 1). For the first 3 modes, in Figure 3, the success rate of the damage localization for the statistical χ_t^2-test is satisfactory only in the interval of the Laplace variables, $s = (p, q) \in \mathbb{C}$ with $p = 1 : 0.5 : -3$ and $q = 8 : 2 : 64$. After that, it is almost flat and cannot indicate the damage position due to modal truncation error in the region $s = (p, q) \in \mathbb{C}$ where $p = 1 : 0.5 : -3$

and $q = 66:2:130$. Note that the considered modes in this example are in the interval $[1,62]$ on the imaginary line (see Table1).

Similarly, for the last 3 modes, it can be seen in Figure 4 that the success rate of damage localization for the statistical χ_t^2-test is high enough in the area of the last two identified poles. In this case, in Figure 4, the good s-values are located in the interval $[102,128]$ on the imaginary line as are the last two identified poles, while there is no success of damage localization around the first four-identified poles because of modal truncation errors. Still, there is a slight bump around the fourth mode. So, choosing the s-value in the vicinity of the identified poles is not always perfect.

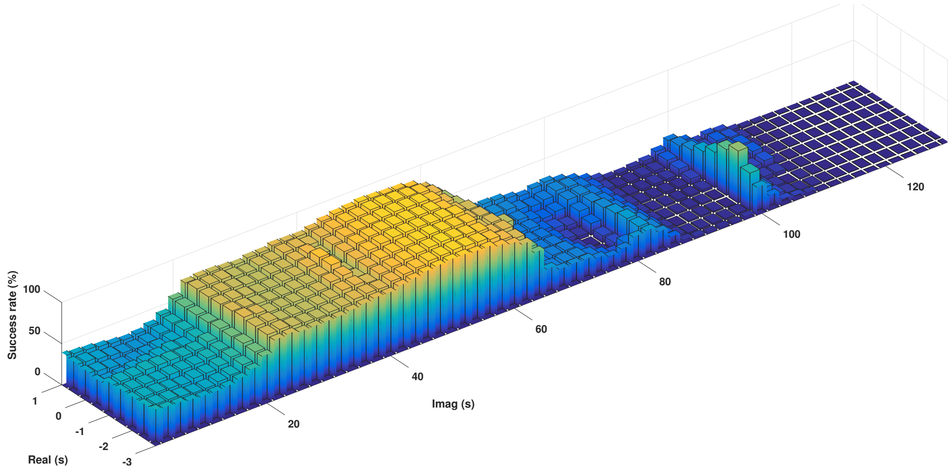

Figure 3: Success rate of the damage localization with statistical evaluation of χ_t^2-test using single mode set i in dependence of s

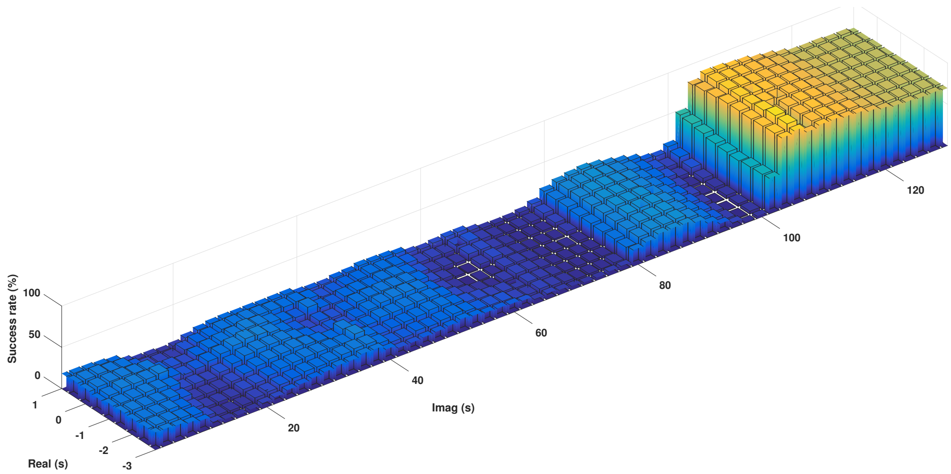

Figure 4: Success rate of the damage localization with statistical evaluation of χ_t^2-test using single mode set j in dependence of s

5.5 Success rate of the damage localization using multiple mode sets

In this section, the new statistical approach is presented using multiple mode sets to increase the success rate of damage localization in the s-plane. Hence, choose the range of the respective s-values s_i and s_j as $(p_i, q_i) \in \mathbb{C}$ and $(p_j, q_j) \in \mathbb{C}$ where $p_i = 1:0.5:-3$, $q_i = 1:2:64$, $p_j = 1:0.5:-3$ and $q_j = 66:2:128$ for the respective mode sets i and j. In the previous section, the success rate of the damage localization with SDDLV was not successful everywhere in the s-plane because of modal truncation and estimation errors. It motivates the use of multiple mode sets instead of using a single mode set alone. Therefore, the computation of stress for damage localization is derived by taking into account the information using multiple mode sets instead of using a single mode set. The joint stress evaluation derived in Section 4 is performed and its joint covariance is computed for multiple mode sets $\mathscr{M} = (i, j)$ containing the first three and last 3 identified poles (see Table 1).

Recall that the optimal choice of the Laplace variable for each mode set depends on the selected modes within this set. Suitable s-values have been found to be in the vicinity of the chosen modes. In the previous experiments, it has been seen that highest success rates of the damage localization are located in the vicinity of the identified poles (see Figures 3 and 4) for the respective mode sets i and j. The impact of choice of s-values s_i and s_j has been investigated differently for the respective mode sets. The following two cases are now considered.

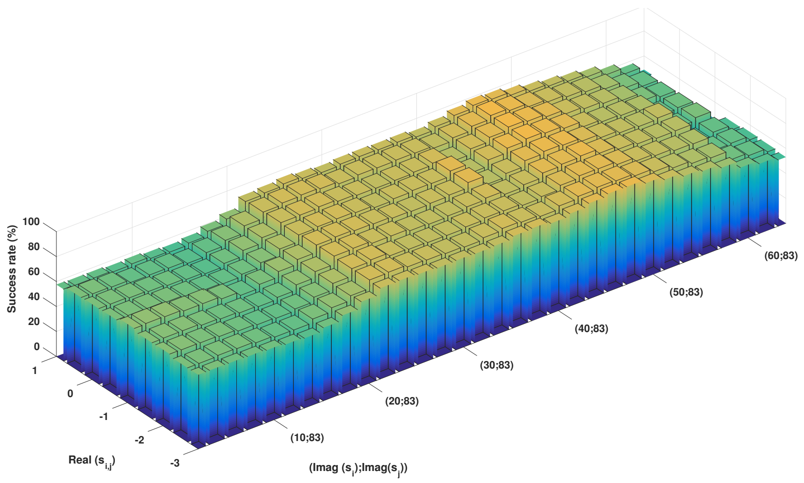

Figure 5: Case 1- Success rate of the damage localization with statistical evaluation of χ_t^2-test using multiple mode sets i, j in dependence of s $[s_i = (1 : 0.5 : -3, 1 : 2 : 64); s_j = (1 : 0.5 : -3, 83)]$

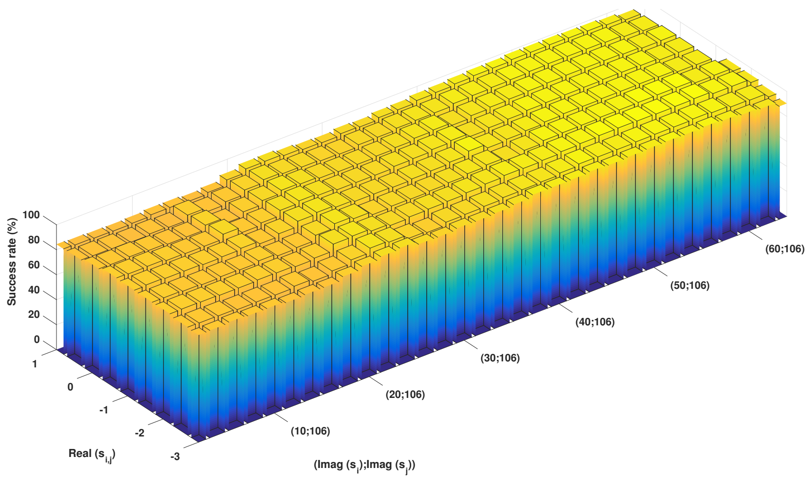

Figure 6: Case 2- Success rate of the damage localization with statistical evaluation of χ_t^2-test using multiple mode sets i, j in dependence of s $[s_i = (1 : 0.5 : -3, 1 : 2 : 64); s_j = (1 : 0.5 : -3, 106)]$

Case 1: the s-value $s_i = (p_i, q_i) \in \mathbb{C}$ has been chosen with $p_i = 1 : 0.5 : -3$ and $q_i = 1 : 2 : 64$ in the vicinity of mode set i, while $s_j = (p_j, q_j) \in \mathbb{C}$ is chosen with $p_j = 1 : 0.5 : -3$ and kept fixed at $q_j = 83$ where it leads to a poor performance for the damage localization in both Figure 3 and Figure 4. In this case, in Figure 5, the maximum success rate is achieved in the region $[s_i = (1 : 0.5 : -3, 22 : 2 :$

62);$s_j = (1:0.5:-3,83)$], which is much larger and achieving higher success rate than both satisfactory region $s(1:0.5:-3,20:2:62)$ in Figure 3 and $s(1:0.5:-3,102:2:128)$ in Figure 4. Notice that the relatively lower rate in region [$s_i = (1:0.5:-3,1:2:20)$;$s_j = (1:0.5:-3,83)$] of Figure 5 is still higher than the very same region in both Figures 3 and 4.

Case 2: the choice of Laplace variable s_i is similar as in case 1 but $s_j = (p_j, q_j) \in \mathbb{C}$ has been chosen with $p_j = 1:0.5:-3$ and kept fixed at $q_j = 106$ such that it corresponds to achieving a good performance of the damage localization in Figure 4. In this case, it has been seen that the success rate of the damage localization with the new method has significantly improved the situation everywhere in the s-plane in Figure 6 compared to all previous results. When considering the statistical uncertainties of the modal parameters using multiple mode sets, the subsequent stress evaluation can improve the situation significantly.

6. CONCLUSIONS

In this paper, the damage localization with SDDLV has been extended considering multiple mode sets. The robustness of damage localization has been obtained by a joint statistical evaluation taking into account the information from all modes on the structure. The stress computation using multiple mode sets increases the information content about the damaged or non-damaged elements of the structure. In the application, several experiments have been carried out to evaluate the success of the damage localization in dependence of the s-value, where all stress values corresponding to an element are being tested for damage in a hypothesis test. The proposed method has increased the success rate of the correct damage localization almost everywhere in the complex s-plane compared to using a single mode set.

ACKNOWLEDGMENTS

Financial support from the Bretagne region is gratefully acknowledged.

REFERENCES

[1] D. Bernal. Load vectors for damage location in systems identified from operational loads. *Journal of Engineering Mechanics*, 136(1):31–39, 2010.

[2] R. Pintelon, P. Guillaume, and J. Schoukens. Uncertainty calculation in (operational) modal analysis. *Mechanical Systems and Signal Processing*, 21(6):2359–2373, 2007.

[3] E. Reynders, R. Pintelon, and G. De Roeck. Uncertainty bounds on modal parameters obtained from stochastic subspace identification. *Mechanical Systems and Signal Processing*, 22(4):948–969, 2008.

[4] E.P. Carden and A. Mita. Challenges in developing confidence intervals on modal parameters estimated for large civil infrastructure with stochastic subspace identification. *Structural Control and Health Monitoring*, 18(1):53–78, 2011.

[5] M. Döhler, L. Marin, D. Bernal, and L. Mevel. Statistical decision making for damage localization with stochastic load vectors. *Mechanical Systems and Signal Processing*, 39(1-2):426–440, 2013.

[6] L. Marin, M. Döhler, D. Bernal, and L. Mevel. Robust statistical damage localization with stochastic load vectors. *Structural Control and Health Monitoring*, 22:557–573, 2015.

[7] M. Döhler and L. Mevel. Efficient multi-order uncertainty computation for stochastic subspace identification. *Mechanical Systems and Signal Processing*, 38(2):346–366, 2013.

[8] D. Bernal. Flexibility-based damage localization from stochastic realization results. *Journal of Engineering Mechanics*, 132(6):651–658, 2006.

[9] D. Bernal. Load vectors for damage localization. *Journal of Engineering Mechanics*, 128(1):7–14, 2002.

[10] D. Bernal. Damage localization from the null space of changes in the transfer matrix. *AIAA Journal*, 45(2):374–381, 2007.

[11] P. Van Overschee and B. De Moor. *Subspace Identification for Linear Systems: Theory, Implementation, Applications*. Kluwer, 1996.

[12] M. Döhler and L. Mevel. Fast multi-order computation of system matrices in subspace-based system identification. *Control Engineering Practice*, 20(9):882–894, 2012.